

THE SCATTERING PHASE: SEEN AT LAST*

JEFFREY GALKOWSKI[†], PIERRE MARCHAND[‡], JIAN WANG[§], AND
MACIEJ ZWORSKI[¶]

Abstract. The scattering phase, defined as $\log \det S(\lambda)/2\pi i$ where $S(\lambda)$ is the (unitary) scattering matrix, is the analogue of the counting function for eigenvalues when dealing with exterior domains and is closely related to Kreĭn’s spectral shift function. We revisit classical results on asymptotics of the scattering phase and point out that it is never monotone in the case of strong trapping of waves. Perhaps more importantly, we provide the first numerical calculations of scattering phases for nonradial scatterers. They show that the asymptotic Weyl law is accurate even at low frequencies and reveal effects of trapping such as lack of monotonicity. This is achieved by using the recent high level multiphysics finite element software FreeFEM.

Key words. scattering phase, obstacle scattering, finite element, Weyl law, trapping

MSC code. 35P25

DOI. 10.1137/23M1547147

1. Introduction. The scattering phase and its close relative, the spectral shift function, have been studied by mathematicians at least since the work of Birman and Kreĭn [BK62]. In the case of radial scattering, the scattering phase is the sum of phase shifts which are a central and classical topic in quantum scattering—see, for instance, [Sa20, section 6.4].

The scattering phase is defined using the scattering matrix, $S(\lambda)$, which is a unitary operator mapping incoming waves to outgoing waves—see section 2 and Figure 3. Because of its structure, the determinant of $S(\lambda)$ is well defined and we put

$$(1.1) \quad \sigma(\lambda) := \frac{1}{2\pi i} \log \det S(\lambda) \in \mathbb{R}, \quad \sigma(0) = 0,$$

where the last condition fixes the choice of \log .

The scattering phase, $\sigma(\lambda)$, is appealing to mathematicians since it is a replacement for the counting function of eigenvalues for scattering problems—see [DyZw19a, sections 2.6, 3.9] and references given there. More precisely, as established by Jensen and Kato [JeKa78] and Bardos, Guillot, and Ralston [BGR82], $\sigma(\lambda)$ satisfies

$$(1.2) \quad \operatorname{tr}(f(-\Delta_{\mathbb{R}^n \setminus \mathcal{O}}) - f(-\Delta)) = \int_0^\infty f(\lambda^2) \sigma'(\lambda) d\lambda, \quad f \in \mathcal{S}(\mathbb{R}).$$

*Received by the editors January 17, 2023; accepted for publication (in revised form) November 10, 2023; published electronically February 12, 2024.

<https://doi.org/10.1137/23M1547147>

Funding: The first author was partially supported by EPSRC Early Career Fellowship EP/V001760/1 and Standard grant EP/V051636/1, the second author was partially supported by EPSRC grant EP/R005591/1, and the fourth author was partially supported by NSF grant DMS-1952939.

[†]Department of Mathematics, University College London, London, WC1H 0AY, UK (j.galkowski@ucl.ac.uk).

[‡]Unité de Mathématiques Appliquées de ENSTA Paris, 91762 Palaiseau Cedex, France (pierre.marchand@inria.fr).

[§]Department of Mathematics, University of North Carolina, Chapel Hill, Chapel Hill, NC 27599 USA (wangjian@email.unc.edu).

[¶]Department of Mathematics, University of California, Berkeley, Berkeley, CA 94720 USA (zworski@berkeley.edu).

Here, as in the rest of this paper, we specialized to the case of Dirichlet Laplacian, $\Delta_{\mathbb{R}^n \setminus \mathcal{O}}$ on $\mathbb{R}^n \setminus \mathcal{O}$, where $\mathcal{O} \Subset \mathbb{R}^n$ is a bounded open set with a piecewise smooth boundary and connected complement. (Strictly speaking, $f(-\Delta_{\mathbb{R}^n \setminus \mathcal{O}})$ and $f(-\Delta)$ are defined on $L^2(\mathbb{R}^n \setminus \mathcal{O})$ and $L^2(\mathbb{R}^n)$, respectively, using the spectral theorem, but we consider the former space as a subspace of $L^2(\mathbb{R}^n)$ using extension by 0.)

It could then be considered somewhat surprising that, to our knowledge, $\sigma(\lambda)$ has only been exhibited for radial scatterers. That is, there has never been any form of an actual assignment, via a numerical approximation, of $\lambda \mapsto \sigma(\lambda)$. (For radial scatterers, the calculation of the scattering phase is classical, appearing, for example, in many physics textbooks, e.g., [Ha13].) At the time when asymptotic formulae for $\sigma(\lambda)$ were mathematically investigated (see section 1.1) it is safe to say that such numerical computations were out of reach. Here we benefit from major advances in computational power and, in particular, from the recent high level multiphysics finite element software FreeFEM—see section 4.

The numerical results for a variety of two-dimensional scatterers \mathcal{O} are shown in our figures. The main conclusions are as follows:

- The Weyl asymptotics for $\sigma(\lambda)$ given in (1.5) provide an accurate approximation starting at 0 energy; this accuracy is particularly striking in the case of nontrapping geometries—see Figure 1. They also appear remarkably accurate in trapping geometries.
- Strong trapping immediately causes lack of monotonicity of $\sigma(\lambda)$ which in accordance with (1.7) is related to the presence of resonances near the real axis (as reviewed in section 1.2)—see Figure 2, top. Here, by strong trapping we mean that a small perturbation of a trapped ray remains trapped.
- Mild trapping, illustrated in the two bottom figures of Figure 2, does not seem to destroy monotonicity but there is a visible effect from scattering resonances at least for low frequencies. We show examples with two types of mild trapping, parabolic and hyperbolic. In parabolic trapping, a perturbation of the trapped rays of size $\sim \epsilon$ escapes in time ϵ^{-1} , while in hyperbolic trapping (the weakest form of trapping), this perturbation escapes in time $\log \epsilon^{-1}$.
- For star-shaped obstacles the scattering phase is monotone [Ra78]. This monotonicity is not known for nontrapping obstacles even though [PePo82] provided full asymptotic expansion for $\sigma(\lambda)$; numerical examples suggest that $\sigma(\lambda)$ may always be monotone for nontrapping obstacles—see Figure 1. More experimentation would, however, be required for a firm conjecture.

1.1. Weyl law for $\sigma(\lambda)$. Possibly the most striking result about the counting function for the eigenvalues of the Dirichlet Laplacian, $\Delta_{\mathcal{O}}$, on a *bounded* domain $\mathcal{O} \subset \mathbb{R}^n$ is the Weyl law is, with

$$(1.3) \quad \begin{aligned} N(\lambda) &:= |\text{Spec}(-\Delta_{\mathcal{O}}) \cap [0, \lambda^2]|, \\ N(\lambda) &= \frac{\omega_n \text{vol}(\mathcal{O})}{(2\pi)^n} \lambda^n - \frac{\omega_{n-1} \text{vol}(\partial\mathcal{O})}{4(2\pi)^{n-1}} \lambda^{n-1} + o(\lambda^{n-1}), \end{aligned}$$

where $\omega_n := \text{vol}(B_{\mathbb{R}^n}(0, 1))$. It was conjectured by Weyl in 1913 and established by Ivrii in 1980 (see [SaVa97] and [Iv16] for the history of this problem) under the assumptions that $\partial\mathcal{O}$ is smooth and the set of periodic orbits has measure zero (a generically valid fact expected to be true for all \mathcal{O} with smooth boundaries).

The trace formula (1.2) shows that $\sigma(\lambda)$ is the exact analogue of $N(\lambda)$ since $\text{tr } f(\Delta_{\mathcal{O}}) = \int_0^\infty f(\lambda^2) N'(\lambda) d\lambda$. It is then natural to ask if (1.3) holds for $\sigma(\lambda)$, with

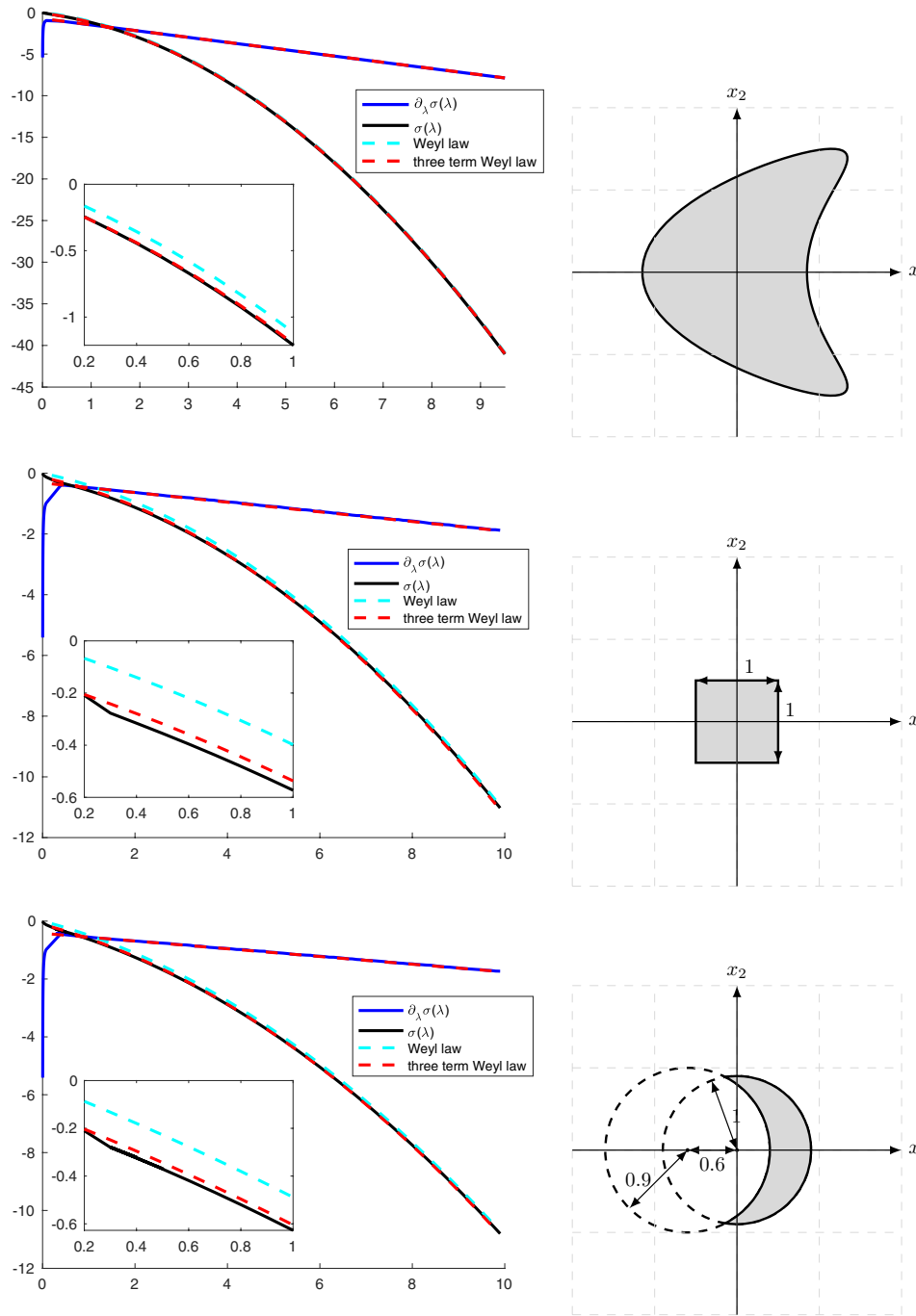


FIG. 1. Scattering phase and the corresponding geometry. From top to bottom: a star-shaped obstacle, a star-shaped obstacle with corners, and a nontrapping nonstar-shaped obstacle. We also indicate the comparisons with the Weyl law (1.5) and the (conjectural) three term Weyl for obstacles with corners (1.6).

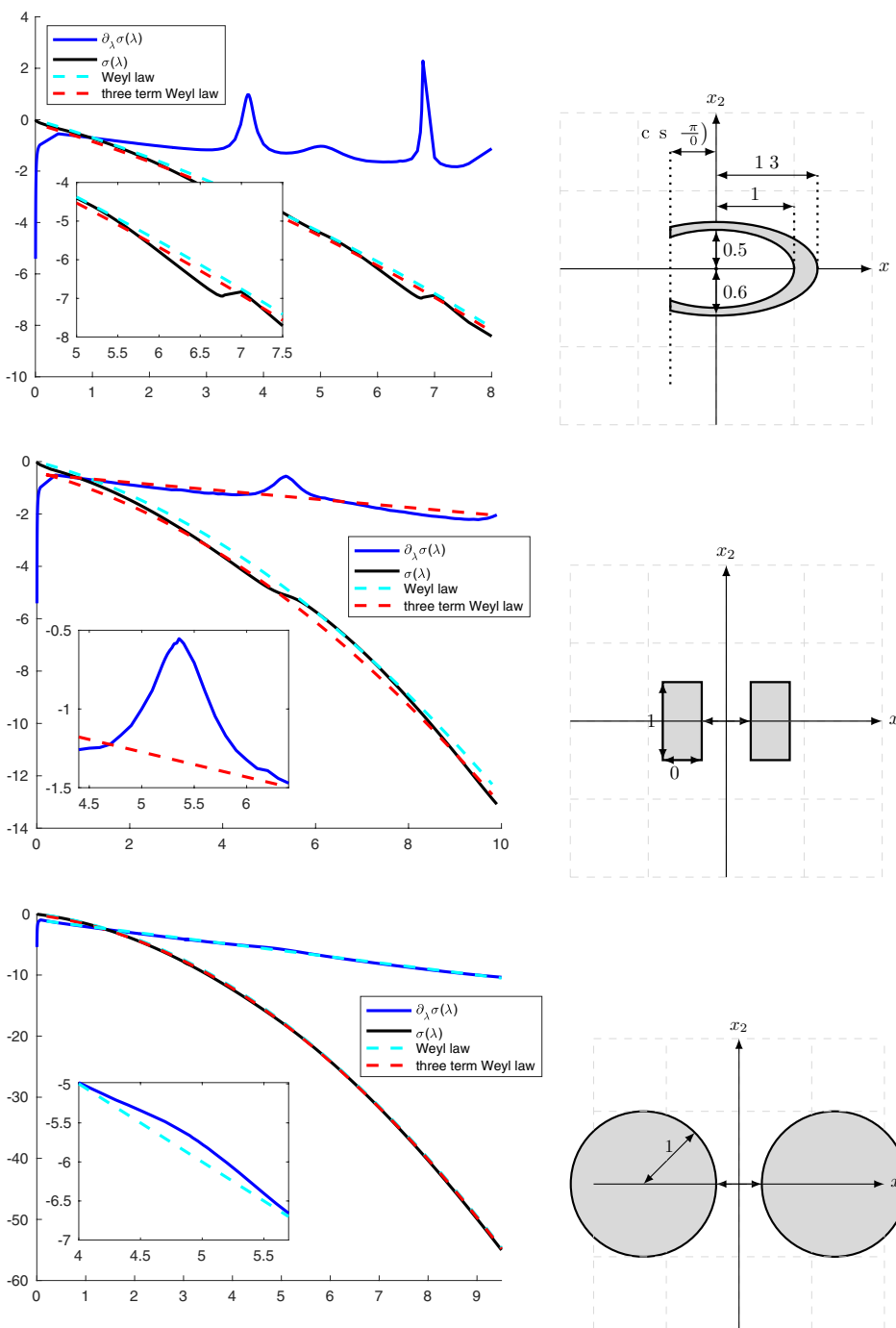


FIG. 2. Scattering phase and the corresponding geometry. From top to bottom: strong trapping in a cavity, parabolic trapping from bouncing ball orbits, and hyperbolic trapping in the form of one closed orbit. In the case of strong trapping, we see numerical manifestations of (1.7). For the two rectangles, we expect resonances with $|\text{Im } \lambda_j| \sim 1/|\lambda_j|$ so that (1.7) is inconclusive. In the case of two or more discs, the resonances satisfy $|\text{Im } \lambda_j| > c$ (see [Va22] and references given there) and, as a result, at high energies their effect is weak. The peaks in the strongly trapping cavity occur at $\lambda \approx 3.78$ and $\lambda \approx 6.85$. This corresponds, roughly, to having $\frac{1}{2}$ or 1 wavelength vertically in the cavity, respectively.

the understanding that in agreement with (1.2) we now consider the renormalized volume of $\mathbb{R}^n \setminus \mathcal{O}$. Hence the natural analogue of (1.3) is given by

$$(1.4) \quad \sigma(\lambda) = -\frac{\omega_n \text{vol}(\mathcal{O})}{(2\pi)^n} \lambda^n - \frac{\omega_{n-1} \text{vol}(\partial\mathcal{O})}{4(2\pi)^{n-1}} \lambda^{n-1} + o(\lambda^{n-1}).$$

The difficulty in obtaining (1.4) stems from the fact that classical Tauberian theorems used for (1.3) use monotonicity of $N(\lambda)$. As we will see in section 1.2, $\sigma(\lambda)$ is *not*, in general, monotone.

However, for star-shaped obstacles $\sigma'(\lambda) \leq 0$ was established by Helton and Ralston [Ra78] (see also [Ka78]). This monotonicity allowed Jensen and Kato [JeKa78] to obtain the leading term in (1.4) in that case (the convex case was treated by Buslaev [Bu75]). For convex obstacles Majda and Ralston [MaRa78a], [MaRa78b], and [MaRa79] improved on [JeKa78] by obtaining a three-term asymptotic expansion of $\sigma(\lambda)$. Using advances in propagation of singularities for obstacle problems (see [HöIII, Chapter 24] and references given there) Petkov and Popov [PePo82] obtained a *full* asymptotic expansion of $\sigma(\lambda)$ as $\lambda \rightarrow \infty$.

The first proof of (1.4) for all obstacles (for which the conditions after (1.3) hold) was given by Melrose [Me88] using his trace formula for scattering poles (see [DyZw19a, sections 3.10, 3.13]). Since that formula holds only in odd dimension, the same restriction was imposed. This restriction was lifted using different methods by Robert [Ro94]. (A proof in all dimensions following Melrose's idea can be given using [PeZw99] and [PeZw00].) In this historical account we only discussed the Dirichlet obstacle case. For more general perturbations see, for instance, [Ch98].

Specialized to two dimensions, (1.4) becomes

$$(1.5) \quad \sigma(\lambda) = -\frac{|\mathcal{O}|}{4\pi} \lambda^2 - \frac{|\partial\mathcal{O}|}{4\pi} \lambda + o(\lambda).$$

In the nontrapping case, in addition to further terms in (1.5), there is an asymptotic formula for $\sigma'(\lambda)$ [PePo82]. When a nontrapping \mathcal{O} has corners (i.e., has piecewise smooth, Lipschitz boundary), the following formula is suggested by heat expansions for interior problems which can be found in [Ch83, MaRo15]:

$$(1.6) \quad \sigma(\lambda) = -\frac{|\mathcal{O}|}{4\pi} \lambda^2 - \frac{|\partial\mathcal{O}|}{4\pi} \lambda + \frac{1}{24} \sum_j \left(\frac{\theta_j}{\pi} - \frac{\pi}{\theta_j} \right) - \frac{1}{24\pi} \int_{\partial\mathcal{O}} H ds + o(1),$$

where θ_j are the angles at the corners (measured from outside) and H is the curvature (with the convention that $H > 0$ for circles; we note that if there are no corners and connected \mathcal{O} , $\int_{\partial\mathcal{O}} H ds = 2\pi$). However, to our knowledge only the first asymptotic term of (1.6) is known rigorously in this case.

In the figures illustrating numerical results both asymptotic formulas are plotted against the computed scattering phase and its derivative. It is interesting to note that for most frequencies $\sigma'(\lambda)$ seems to agree with the asymptotic formula given by formal differentiation of (1.5) even in trapping cases. This is similar to phenomena proved in the recent work of Lafontaine, Spence, and Wunsch [LSW21] and perhaps could be rigorously established by similar methods.

1.2. Breit–Wigner approximation at high energies. Scattering resonances, which replace discrete spectral data for problems on unbounded domains, can be defined (in obstacle scattering) as poles of the meromorphic continuation of $S(\lambda)$ —see [DyZw19a, section 4.4]. Since $S(\lambda)$, $\lambda > 0$ captures observable phenomena, it is

interesting to see how those (complex) poles manifest themselves in its behavior. The Breit–Wigner formula (see [DyZw19a, section 2.2]) is one such way. In high energy obstacle scattering it was proved by Petkov and Zworski [PeZw99] and [PeZw00] and takes the following form:

$$(1.7) \quad \sigma'(\lambda) = \sum_{|\lambda_j - \lambda| < 1} \frac{1}{\pi} \frac{|\operatorname{Im} \lambda_j|}{|\lambda - \lambda_j|^2} + \mathcal{O}(\lambda^{n-1}),$$

where λ_j 's are the scattering resonances, that is, the poles of $S(\lambda)$. From the point of view of the scattering asymptotics (1.4) we note that the sign of the Breit–Wigner terms (the sum of Lorentzians on the right in (1.7)) is opposite of the overall trend. In particular, if there exist λ_j 's with $|\operatorname{Im} \lambda_j| \ll (\operatorname{Re} \lambda_j)^{1-n}$, then $\sigma'(\lambda) > 0$ for λ near $\operatorname{Re} \lambda_j$. Strong trapping, such as that shown in Figure 2 (top figure), is known to produce resonances with $\operatorname{Im} \lambda_j = \mathcal{O}(|\lambda_j|^{-\infty})$ —see [St99], [TZ98]. Consequently, whenever such strong trapping occurs the scattering phase is *not* monotone.

The strong and parabolic trapping examples in Figure 2 (top two figures) show the presence of Lorentzians in σ' already at low energies. In the very weak trapping illustrated in the bottom of Figure 2 there is some evidence of a low energy resonance but the effect seems minimal.

1.3. Low energy asymptotics. The numerical methods used to compute $\sigma'(\lambda)$ are not effective at very low energies—see section 4. To obtain $\sigma(\lambda)$ by integration we used low energy asymptotic formulae for $\sigma'(\lambda)$. There has been recent progress on this subject and it is natural to review it here.

The first result we are aware of was obtained by Hassell and Zelditch [HaZe99] (using monotonicity of $\sigma(\lambda)$ as a function of the obstacle [Ra78]) and stated that $\sigma(\lambda) \sim \frac{1}{2} \log \lambda$. That was a by-product of their work on planar obstacles with the same scattering phase (an analogue of the isospectral problem). This result was successively improved by McGillivray [McG13], Strohmaier and Waters [StWa20], and Christiansen and Datchev [ChDa22] and a more precise asymptotic formula is given by

$$(1.8) \quad \sigma'(\lambda) \sim -\frac{2}{\lambda} \frac{1}{(-2 \log 2\lambda + C(\mathcal{O}) + 2\gamma)^2 + \pi^2}$$

with $C(\mathcal{O})$ the logarithmic capacity of \mathcal{O} (see below) and γ the Euler constant. One way to define $C(\mathcal{O})$ is to consider the Green function of \mathcal{O} :

$$-\Delta G(x) = 0, \quad x \in \mathbb{R}^2 \setminus \mathcal{O}, \quad G(x) = 0, \quad x \in \partial \mathcal{O}, \quad G(x) \sim \log |x|, \quad |x| \rightarrow \infty.$$

Then

$$G(x) = \log |x| - C(\mathcal{O}) + o(1), \quad |x| \rightarrow \infty.$$

We used the leading term of the low energy asymptotics to enhance the numerics. Indeed, the method described below numerically approximates $\sigma'(\lambda)$ and is then integrated to obtain $\sigma(\lambda)$. Since our numerical computation of $\sigma'(\lambda)$ is not accurate for $0 < \lambda \ll 1$, in the integration step we instead use the leading small λ asymptotics when $\lambda \ll 1$.

2. A formula for the derivative of the scattering phase. In order to compute $\sigma(\lambda)$ we recall a definition of the scattering matrix in dimension $n = 2$; for motivation and a detailed presentation see [DyZw19a, sections 3.7, 4.4].

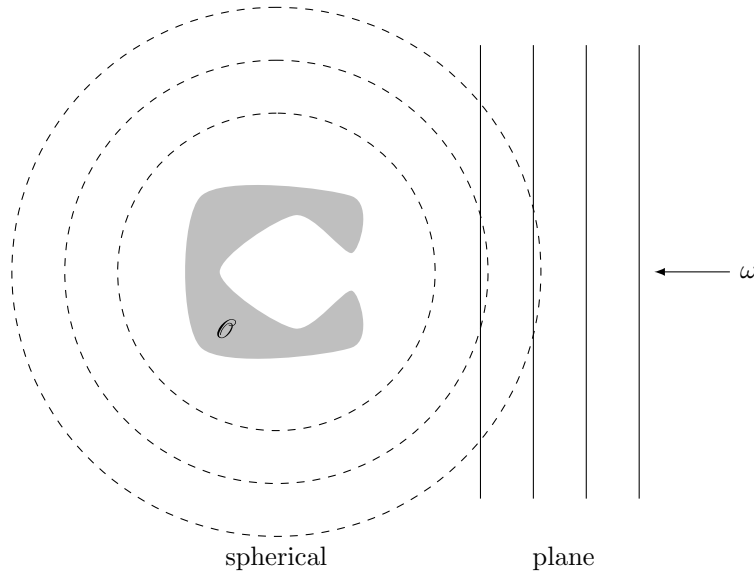


FIG. 3. The waves used to define the scattering matrix.

We start with perturbed plane waves; see (2.3) below. For that we let $\omega \in \mathbb{S}^1$, $\lambda \in \mathbb{R}$ and define $u(\lambda, \cdot, \omega) \in C^\infty(\mathbb{R}^2)$ as the unique *outgoing* solution to

$$(2.1) \quad (-\Delta - \lambda^2)u = 0 \text{ in } \mathbb{R}^2 \setminus \mathcal{O}, \quad u|_{\partial\mathcal{O}} = -e^{i\lambda\langle x, \omega \rangle}|_{\partial\mathcal{O}}.$$

(We note that, to streamline notation, the convention is slightly different than in [DyZw19a].) Here, by *outgoing*, we mean that there is $b(\lambda, \cdot, \omega) \in C^\infty(\mathbb{S}^1)$ such that

$$(2.2) \quad u(\lambda, x, \omega) = e^{-\frac{\pi i}{4}} \sqrt{2\pi/(\lambda|x|)} e^{i\lambda|x|} b(\lambda, x/|x|, \omega) + O(|x|^{-3/2}).$$

Remark. There is a corresponding notion of an *incoming* solution where $e^{i\lambda|x|}$ is replaced by $e^{-i\lambda|x|}$ in (2.2). All solutions to (2.1) can then be written as linear combinations of these two types of solutions.

We then define

$$(2.3) \quad e(\lambda, x, \omega) := e^{i\lambda\langle x, \omega \rangle} + u(\lambda, x, \omega).$$

The scattering matrix, $S(\lambda) : L^2(\mathbb{S}^1) \rightarrow L^2(\mathbb{S}^1)$, is then given by $S(\lambda) := I + A(\lambda)$, where $A(\lambda)$ is an integral operator defined as

$$(2.4) \quad A(\lambda)f(\theta) := \int_{\mathbb{S}^1} A(\lambda, \theta, \omega) f(\omega) d\omega, \quad A(\lambda, \theta, \omega) := b(\lambda, \theta, \omega).$$

The scattering matrix $S(\lambda)$ is unitary and extends meromorphically to the Riemann surface of $\log \lambda$.

It will be useful when computing the scattering phase to rewrite the integral kernel $A(\lambda, \theta, \omega)$ as an integral over $\partial\mathcal{O}$.

LEMMA 1. Let ν denote unit normal to $\partial\mathcal{O}$ pointing out of \mathcal{O} . Then, in the notation of (2.3), we have (with $ds(x)$ the line measure on $\partial\mathcal{O}$ or $\partial B(0, r)$)

$$(2.5) \quad A(\lambda, \theta, \omega) = \frac{1}{4\pi i} \int_{\partial\mathcal{O}} e^{-i\lambda\langle x, \theta \rangle} \partial_\nu e(\lambda, x, \omega) ds(x).$$

Proof. Green’s formula shows that, with $e(x) := e(\lambda, x, \omega)$ and $\mathcal{O} \subset B(0, R)$,

$$\begin{aligned}
 (2.6) \quad 0 &= \int_{B(0,R) \setminus \mathcal{O}} \left([(-\Delta - \lambda^2)e(x)](e^{-i\lambda\langle x, \theta \rangle}) - e(x)[(-\Delta - \lambda^2)e^{-i\lambda\langle x, \theta \rangle}] \right) dx \\
 &= \int_{\partial \mathcal{O}} e^{-i\lambda\langle x, \theta \rangle} \partial_\nu e(x) ds(x) - \int_{\partial B(0,R)} \left(\partial_r e(x) e^{-i\lambda\langle x, \theta \rangle} - e(x) \partial_r [e^{-i\lambda\langle x, \theta \rangle}] \right) ds(x).
 \end{aligned}$$

To compute the last term in (2.6), we use the formulae (2.2) and (2.3) together with the stationary phase method (see [DyZw19a, Theorem 3.38]): for $a \in C^\infty(\mathbb{S}^1)$,

$$\begin{aligned}
 (2.7) \quad \int_{\partial B(0,R)} a(x/|x|) e^{-i\lambda\langle x, \theta \rangle} ds(x) &= \sqrt{2\pi R/\lambda} (e^{-\frac{i\pi}{4}} a(-\theta) e^{i\lambda R} + e^{\frac{i\pi}{4}} a(\theta) e^{-i\lambda R}) \\
 &\quad + \mathcal{O}(R^{-\frac{1}{2}}).
 \end{aligned}$$

By applying (2.7) when $\theta \neq \omega$, and the $x \mapsto -x$ symmetry when $\omega = \theta$, we obtain $\int_{\partial B(0,R)} \langle x/|x|, \omega + \theta \rangle e^{i\lambda\langle x, \omega - \theta \rangle} ds(x) = \mathcal{O}(R^{-\frac{1}{2}})$. This and (2.3) give, with $u(x) := u(\lambda, x, \omega)$,

$$\begin{aligned}
 &\int_{\partial B(0,R)} \left(\partial_r e(x) e^{-i\lambda\langle x, \theta \rangle} - e(x) \partial_r [e^{-i\lambda\langle x, \theta \rangle}] \right) ds(x) \\
 &= \int_{\partial B(0,R)} (\partial_r u(x) + i\lambda \langle x/|x|, \theta \rangle u(x)) e^{-i\lambda\langle x, \theta \rangle} ds(x) + \mathcal{O}(R^{-\frac{1}{2}}).
 \end{aligned}$$

In the notation of (2.2), we put $B := e^{-\pi i/4} \sqrt{2\pi/\lambda} b(\lambda, x/|x|, \omega)$ and then apply (2.7) to see that this expression is equal to

$$\begin{aligned}
 e^{i\lambda R} R^{-\frac{1}{2}} \int_{\partial B(0,R)} (i\lambda + i\lambda \langle x/|x|, \theta \rangle) B e^{-i\lambda\langle x, \theta \rangle} ds(x) + \mathcal{O}(R^{-\frac{1}{2}}) &= 4\pi i b(\lambda, \theta, \omega) \\
 &\quad + \mathcal{O}(R^{-\frac{1}{2}}).
 \end{aligned}$$

Combined with (2.6) and (2.4) this completes the proof of (2.5) by taking $R \rightarrow \infty$. \square

Remarks.

1. For evaluating the traces in Lemma 2 numerically we note that, using a positive parametrization $[0, L] \rightarrow \partial \mathcal{O}$, $s \mapsto x = x(s)$, $|\dot{x}| = 1$, $\nu(s) = (\dot{x}_2(s), -\dot{x}_1(s))$ (ν is the outward normal),

$$\begin{aligned}
 (2.8) \quad \partial_\nu (e^{i\lambda\langle x, \omega \rangle}) &= i\lambda \langle \dot{x}, \omega^\perp \rangle e^{i\lambda\langle x, \omega \rangle}, \\
 \mathbb{S}^1 \ni \omega = (\cos t, \sin t), \quad \omega^\perp &:= (-\sin t, \cos t), \quad t \in [0, 2\pi).
 \end{aligned}$$

2. We recall the following symmetry of $e(\lambda, x, \omega)$ [DyZw19a, Theorem 4.20]:

$$\overline{e(\lambda, x, \omega)} = e(-\lambda, x, \omega).$$

3. Note that although $\partial \mathcal{O}$ may have corners in our examples, since the boundary is piecewise smooth and Lipschitz, the formula (2.5) makes sense and remains valid.

Next, we calculate a formula for $\sigma'(\lambda)$ in terms of $e(\lambda, x, \omega)$. The definitions give

$$(2.9) \quad \sigma'(\lambda) = \frac{1}{2\pi i} \operatorname{tr} S(\lambda)^* \partial_\lambda S(\lambda) = \frac{1}{2\pi i} \operatorname{tr} \partial_\lambda A(\lambda) + \frac{1}{2\pi i} \operatorname{tr} A(\lambda)^* \partial_\lambda A(\lambda).$$

We start with the first term on the right-hand side of (2.9).

LEMMA 2. *We have*

$$(2.10) \quad \operatorname{tr} \partial_\lambda A(\lambda) = \frac{1}{4\pi} \int_{\mathbb{S}^1} \int_{\partial\mathcal{O}} e^{-i\lambda\langle x, \omega \rangle} G(\lambda, x, \omega) ds(x) d\omega,$$

where, in the notation of (2.3),

$$(2.11) \quad \begin{aligned} G(\lambda, x, \omega) &:= -\langle x, \omega \rangle \partial_\nu u(\lambda, x, \omega) + \partial_\nu v(\lambda, x, \omega), \\ (-\Delta - \lambda^2)v(\lambda, x, \omega) &= -2i\lambda u(\lambda, x, \omega), \quad x \in \mathbb{R}^2 \setminus \mathcal{O}, \\ v(\lambda, x, \omega)|_{\partial\mathcal{O}} &= -\langle x, \omega \rangle e^{i\lambda\langle x, \omega \rangle}|_{\partial\mathcal{O}}. \end{aligned}$$

Proof. The integral kernel of $\partial_\lambda A(\lambda)$ is given by

$$(2.12) \quad \partial_\lambda A(\lambda, \theta, \omega) = \frac{1}{4\pi i} \int_{\partial\mathcal{O}} \left(\partial_\lambda [e^{-i\lambda\langle x, \theta \rangle}] \partial_\nu e(\lambda, x, \omega) + e^{-i\lambda\langle x, \theta \rangle} \partial_\nu \partial_\lambda e(\lambda, x, \omega) \right) ds(x).$$

From (2.3) we see that $\partial_\lambda e(\lambda, x, \omega) = i\langle x, \omega \rangle e^{i\lambda\langle x, \omega \rangle} + iv(\lambda, x, \omega)$, where v is defined in the statement of the lemma. Hence, in the notation of (2.8), and with $e := e(\lambda, x, \omega)$, the integrand in (2.12) for $\theta = \omega$ is given by

$$i\langle \dot{x}, \omega^\perp \rangle + i(-\langle x, \omega \rangle \partial_\nu u(\lambda, x, \omega) + \partial_\nu v(\lambda, x, \omega)) e^{-i\lambda\langle x, \omega \rangle}.$$

This gives (2.10) since $\int_{\partial\mathcal{O}} \langle \dot{x}, \omega^\perp \rangle ds = 0$. □

We now move to the second term in (2.9).

LEMMA 3. *We have*

$$(2.13) \quad \operatorname{tr} A(\lambda)^* \partial_\lambda A(\lambda) = \frac{1}{16\pi^2} \int_{\mathbb{S}^1} \int_{\mathbb{S}^1} H(\lambda, \omega, \theta) F(\lambda, \omega, \theta) d\omega d\theta,$$

where in the notation of Lemma 2,

$$\begin{aligned} H &:= \int_{\partial\mathcal{O}} e^{i\lambda\langle x, \theta \rangle} \left(-i\lambda \langle \dot{x}, \omega^\perp \rangle e^{-i\lambda\langle x, \omega \rangle} + \overline{\partial_\nu u(\lambda, x, \omega)} \right) ds(x), \\ F &:= \int_{\partial\mathcal{O}} e^{-i\lambda\langle y, \theta \rangle} \left[(\langle \dot{y}, \omega^\perp \rangle (\lambda \langle y, \theta - \omega \rangle + i) e^{i\lambda\langle y, \omega \rangle} - i \langle y, \theta \rangle \partial_\nu u(\lambda, y, \omega) \right. \\ &\quad \left. + i \partial_\nu v(\lambda, y, \omega) \right] ds(y). \end{aligned}$$

Proof. The integral kernel of $A(\lambda)^*$ is given by

$$A^*(\lambda, \omega, \theta) = -\frac{1}{4\pi i} \int_{\partial\mathcal{O}} e^{i\lambda\langle x, \theta \rangle} \partial_\nu \overline{e(\lambda, x, \omega)} ds(x),$$

and hence $\operatorname{tr} A(\lambda)^* \partial_\lambda A(\lambda)$ is given as an integral over $\partial\mathcal{O}_x \times \partial\mathcal{O}_y \times \mathbb{S}_\theta^1 \times \mathbb{S}_\omega^1$ of

$$\frac{1}{16\pi^2} e^{i\lambda\langle x-y, \theta \rangle} \overline{\partial_\nu e(\lambda, x, \omega)} (-i \langle y, \theta \rangle \partial_\nu e(\lambda, y, \omega) + \partial_\nu \partial_\lambda e(\lambda, y, \omega)).$$

Using $\partial_\lambda e(\lambda, x, \omega) = i\langle x, \omega \rangle e^{i\lambda\langle x, \omega \rangle} + iv(\lambda, x, \omega)$ and the definition of $e(\lambda, x, \omega)$ completes the proof. □

Remark. The integral over θ could be eliminated using Bessel functions. That, however, introduces factors $J_0(\lambda|x-y|)$ and $\langle y, x-y \rangle J_1(\lambda|x-y|)/|x-y|$ and destroys the product structure which only requires separate integration in x and y . Hence, it is not numerically advantageous.

3. Analytic solution for the disc. In order to validate our numerical scheme, the scheme was tested against the analytic solution for \mathcal{O} given by the unit disk. We record in this section the formulae for both $\sigma(\lambda)$ and $u(\lambda, x, \omega)$ in this case.

3.1. The scattering phase for the unit disk. To compute the scattering phase for the disk, we use polar coordinates and separation of variables to find the scattering matrix. In particular, in polar coordinates (r, θ) , a solution to $(-\Delta - \lambda^2)u = 0$ with $u|_{\partial B(0,1)}$ with $u(r, \theta) = \sum_n e^{in\theta} u_n(r)$ satisfies

$$\left(-\partial_r^2 - \frac{1}{r}\partial_r u + \frac{n^2}{r^2} - \lambda^2\right)u_n(r) = 0, \quad u_n(1) = 0,$$

and hence

$$(3.1) \quad u_n(r) = A_n \left(-\frac{H_{|n|}^{(2)}(\lambda)}{H_{|n|}^{(1)}(\lambda)} H_{|n|}^{(1)}(\lambda r) + H_{|n|}^{(2)}(\lambda r) \right).$$

Recall [DLMF, section 10.17(i)] that for $\lambda, r > 0$, $n \geq 0$, we have

$$H_n^{(1)}(\lambda r) = \left(\frac{2}{\pi \lambda r}\right)^{1/2} e^{i(\lambda r - \frac{1}{2}n\pi - \frac{1}{4}\pi)} + O(r^{-3/2}),$$

$$H_n^{(2)}(\lambda r) = \left(\frac{2}{\pi \lambda r}\right)^{1/2} e^{-i(\lambda r - \frac{1}{2}n\pi - \frac{1}{4}\pi)} + O(r^{-3/2}).$$

Thus, $H_{|n|}^{(1)}(\lambda r)$ is outgoing and $H_{|n|}^{(2)}(\lambda r)$ is incoming and hence this implies that $\sin(n\theta)$ ($n \neq 0$) and $\cos(n\theta)$ are eigenfunctions of $S(\lambda)$ with eigenvalue

$$\mu_n := (-1)^{n+1} \frac{H_{|n|}^{(2)}(\lambda)}{H_{|n|}^{(1)}(\lambda)}.$$

In particular, using the Wronskian relation [DLMF, (10.5.5)] in the last line, we obtain

$$(3.2) \quad \begin{aligned} \sigma'(\lambda) &= \left(\frac{1}{2\pi i} \log \det S(\lambda)\right)' \\ &= \frac{1}{2\pi i} \sum_{n=-\infty}^{\infty} \frac{(H_{|n|}^{(2)})'(\lambda)}{H_{|n|}^{(2)}(\lambda)} - \frac{(H_{|n|}^{(1)})'(\lambda)}{H_{|n|}^{(1)}(\lambda)} \\ &= -\frac{2}{\pi^2 \lambda} \sum_{n=-\infty}^{\infty} \frac{1}{H_{|n|}^{(1)}(\lambda) H_{|n|}^{(2)}(\lambda)}. \end{aligned}$$

Remark. Note that we do not write $\sigma(\lambda)$ directly since this would involve making a choice of branch for the logarithm. We instead use $\sigma(0) = 0$ to make this choice when integrating $\sigma'(\lambda)$.

3.2. The scattering amplitude for the unit disk. The incoming portion of $e(\lambda)$ in (2.3) is given by the incoming portion of $e^{i\lambda\langle x, \omega \rangle}$. Using the Jacobi–Anger expansion, with $x = r(\cos \theta, \sin \theta)$ we have

$$\begin{aligned} e^{i\lambda\langle x, \omega \rangle} &= e^{i\lambda r(\cos \theta \cos \omega + \sin \theta \sin \omega)} = e^{i\lambda r \cos(\theta - \omega)} \\ &= \sum_{n=0}^{\infty} \delta_n i^n (H_n^{(1)}(\lambda r) + H_n^{(2)}(\lambda r)) \cos(n(\theta - \omega)), \end{aligned}$$

where $\delta_0 = \frac{1}{2}$ and $\delta_n = 1$ for $n > 0$. Thus, from (3.1) we have

$$e(\lambda, r\theta, \omega) = \sum_{n=0}^{\infty} \delta_n i^n \left(-\frac{H_n^{(2)}(\lambda)}{H_n^{(1)}(\lambda)} H_n^{(1)}(\lambda r) + H_n^{(2)}(\lambda r) \right) \cos(n(\theta - \omega)),$$

and hence

$$(3.3) \quad u(\lambda, r\theta, \omega) = \sum_{n=0}^{\infty} \delta_n i^n \left(1 - \frac{H_n^{(2)}(\lambda)}{H_n^{(1)}(\lambda)} \right) H_n^{(1)}(\lambda r) \cos(n(\theta - \omega)).$$

We can now easily deduce explicit expression for v , $\partial_\nu u$, and $\partial_\nu v$.

4. Numerical scheme. In this section we describe the numerical scheme used to compute the scattering phase.

4.1. Setup. To compute (2.10) and (2.13), we use the trapezoidal rule to approximate the one-dimensional integrals along the angles θ and ω : for $N > 0$, $\omega_l = 2\pi l/N$ for $l = 0 \cdots N-1$. Using 2π -periodicity, we thus arrive at the approximation

$$\text{tr } \partial_\lambda A \approx \frac{1}{4\pi} \frac{2\pi}{N} \sum_{l=0}^{N-1} \int_{\partial\mathcal{O}} e^{-\lambda(\omega_l, x)} G(\lambda, x, \omega_l) ds(x),$$

where G is given in (2.11). For the second term we benefit from the factorization in which we only compute two integrals over the boundary:

$$\text{tr } A^* \partial_\lambda A \approx \frac{1}{16\pi^2} \left(\frac{2\pi}{N} \right)^2 \sum_{l=0}^{N-1} \sum_{p=0}^{N-1} H(\lambda, \omega_l, \theta_p) F(\lambda, \omega_l, \theta_p),$$

where H and F are given in Lemma 3. It remains to compute the normal derivatives of $u(\lambda, \cdot, \omega)$ and $v(\lambda, \cdot, \omega)$ for $\omega \in (\omega_l)_{l=0}^{N-1}$.

To approximate u and v , we first need to reformulate both problems on a bounded domain in $\mathbb{R}^2 \setminus \bar{\mathcal{O}}$. We use the method of *perfectly matched layers* (PML) (introduced in [Be1994] for electromagnetic waves) to do this. More precisely, we use a radial PML [CoMo98]: considering a disk $B_{R_{\text{PML}}}$ with $R_{\text{PML}} > R_{\text{DOM}}$ such that $\bar{\mathcal{O}} \subsetneq B_{R_{\text{DOM}}}$, (see Figure 4) we reformulate both (2.1) and (2.11) using polar coordinates (r, θ) in $B_{R_{\text{PML}}}$, and we apply a complex scaling $\hat{r} = r + \frac{i}{\lambda} \int_0^r \gamma(s) ds$ where γ is an increasing function defined on $[0, R_{\text{PML}})$ and equal to zero in $[0, R_{\text{DOM}})$. Several choices can be made for γ ; we choose $\gamma(r) := 1/(R_{\text{PML}} - r)$ for $r \in [R_{\text{DOM}}, R_{\text{PML}})$ as advocated in [Ber*98]. We denote \mathbf{J}_{PML} the Jacobian of the transformation from the Cartesian coordinates to the complexified Cartesian coordinates.

The equations for u and v , (2.1) and (2.11), are solved with the Galerkin method using Lagrange finite elements; i.e., we solve these equations in a finite-dimensional subspace $V_h \subset H^1(B_{R_{\text{PML}}} \setminus \bar{\mathcal{O}})$ formed by piecewise-polynomial functions on a mesh, and we denote h the mesh element size (see [ErGu22] for more information): we find $u_h, v_h \in V_h$ such that $u_h|_{\partial\mathcal{O}} = -\mathcal{I}_h(e^{i\lambda(x, \omega)})|_{\partial\mathcal{O}}$, $v_h|_{\partial\mathcal{O}} = -\mathcal{I}_h(\lambda \langle x, \omega \rangle e^{i\lambda(x, \omega)})|_{\partial\mathcal{O}}$, where $\mathcal{I}_h : C^0(B_{R_{\text{PML}}} \setminus \bar{\mathcal{O}}) \rightarrow V_h$ is the Lagrange interpolation operator, $u_h|_{\partial B_{\text{PML}}} = v_h|_{\partial B_{\text{PML}}} = 0$,

$$a(u_h, w_h) = 0 \text{ for all } w_h \in V_{h,0}, \text{ and } a(v_h, w_h) = b_{u_h}(w_h) \text{ for all } w_h \in V_{h,0},$$

where $V_{h,0}$ is the subspace of functions in V_h whose value on $\partial\mathcal{O} \cup \partial B_{\text{PML}}$ is zero,

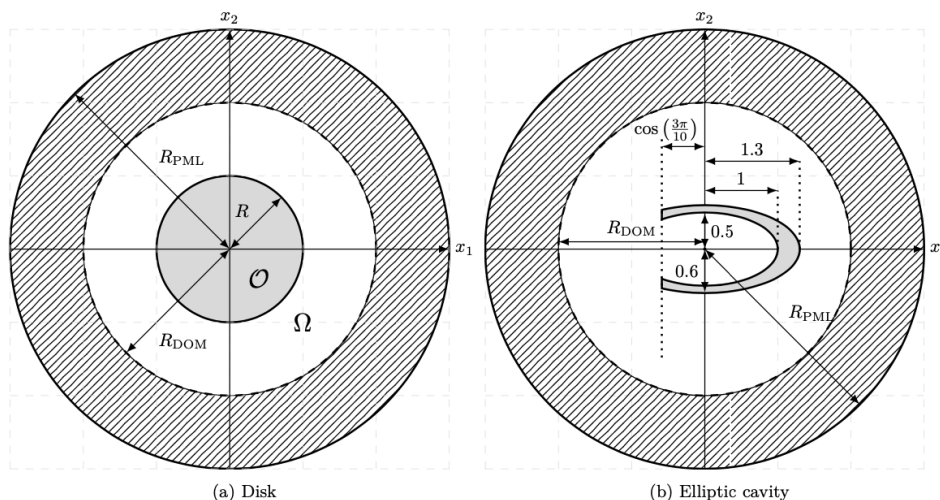


FIG. 4. Considered geometries with their PML.

$$\begin{aligned}
 a(u, w) &= \int_{B_{R_{\text{DOM}}} \setminus \bar{\mathcal{O}}} (\nabla u \cdot \nabla w - \lambda^2 u w) dx dy \\
 &\quad + \int_{B_{R_{\text{PML}}} \setminus \bar{B}_{R_{\text{DOM}}}} (\mathbf{J}_{\text{PML}}^{-T} \nabla u \cdot \mathbf{J}_{\text{PML}}^{-T} \nabla w - \lambda^2 u w) |\det \mathbf{J}_{\text{PML}}| dx dy, \\
 b_{u_h}(w) &= -2i\lambda \int_{B_{R_{\text{PML}}}} u_h w |\det \mathbf{J}_{\text{PML}}| dx dy.
 \end{aligned}$$

In our numerical experiments, the approximation space V_h is spanned by \mathbb{P}_2 Lagrange elements, i.e., continuous piecewise quadratic functions. To bound the error from discretization independently of λ when solving (2.1) and (2.11), we need $h^{2p}\lambda^{2p+1} = h^4\lambda^5$ bounded [DuWu15], where h is the mesh size and p is the degree of the finite element functions. To satisfy this condition, we set the number of points per wavelength to $\mu \times (1 + \lambda^{1/4})$, where μ is a constant. Differentiating u_h and v_h to take the Neumann trace on $\partial\mathcal{O}$, we obtain \mathbb{P}_1 Lagrange elements on the discretization of $\partial\mathcal{O}$, which can then be used to compute $G(\lambda, x, \omega_l)$, $H(\lambda, \omega_l, \theta_p)$, and $F(\lambda, \omega_l, \theta_p)$.

Note that these approximations depend on λ and the angle w_l in the Dirichlet conditions, and thus require solving (2.1) and (2.11) for N different angles and hence N different right-hand sides, for a given frequency λ . Thus, for a given λ , we factorize the matrix stemming from the discretization (note that it is the same for both u_h and v_h), and we use it to solve the discretized problems with several right-hand sides at the same time to improve efficiency. The numerical computations were carried out with FreeFEM [He12]. More precisely, we used its interface with PETSc [Ba*19] to solve linear systems with MUMPS [Am*01, Am*06].

Remark. Since we only need the Neumann traces of u and v to compute the scattering phase, it is quite natural to want to reformulate both problems (2.1) and (2.11) using boundary integral equations (BIEs). While (2.1) can easily be reformulated with a standard BIE, the presence of a right-hand side in (2.11) makes it less convenient

TABLE 1
Relative error on σ' for a disk with $R_{\text{DOM}} = 2$ and $N = 100$.

μ	Relative error on σ'
1	0.1519
5	0.0120
10	0.0038
15	0.0023
20	0.0015
$\lambda = 10, R_{\text{PML}} - R_{\text{DOM}} = 0.25$	
μ	Relative error on σ'
1	0.0258
5	0.0097
10	0.0030
15	0.0016
20	0.0008
$\lambda = 20, R_{\text{PML}} - R_{\text{DOM}} = 0.25$	
μ	Relative error on σ'
1	0.0779
5	0.0108
10	0.0038
15	0.0021
20	0.0015
$\lambda = 10, R_{\text{PML}} - R_{\text{DOM}} = 5h$	
μ	Relative error on σ'
1	0.0334
5	0.0096
10	0.0030
15	0.0015
20	0.0008
$\lambda = 20, R_{\text{PML}} - R_{\text{DOM}} = 5h$	

to usual boundary integral formulations. Nevertheless, it should be possible to represent v differentiating Green's third identity (which we can use to represent u), but it would imply nonstandard boundary integral operators. Thus, we preferred to use more standard tools such as PML.

4.2. Convergence. When \mathcal{O} is a disk, we use the analytical expression from (3.2), with a truncated sum using $|n| \leq 5\lambda$, to compute the relative error on σ' . In Table 1, from left to right, the frequency λ is increasing. The tables at the top have $R_{\text{PML}} - R_{\text{DOM}} = 0.25$, while the tables at the bottom keep a number of mesh cells in the PML region constant, $R_{\text{PML}} - R_{\text{DOM}} = 5h$.

For a fixed $R_{\text{PML}} - R_{\text{DOM}}$ and λ increasing (tables at the top in Table 1), the error is decreasing, which is consistent with [GLS21], which states that the error on u should decrease in this case. We also observed that keeping a fixed number of mesh cells in the PML region (tables at the bottom in Table 1) is enough to have the same level of precision as with a fixed PML region. This is due to the particular choice of γ , and we do not observe this behavior with other usual complex scaling (taking γ as a linear or quadratic function, for example). The advantage is that, in this case, $R_{\text{PML}} - R_{\text{DOM}}$ decreases so that the computational cost is reduced compared to keeping $R_{\text{PML}} - R_{\text{DOM}}$ constant.

TABLE 2
Relative error on σ' for a disk with $R_{\text{DOM}} = 2$ and $R_{\text{PML}} - R_{\text{DOM}} = 5h$.

μ	N	Relative error on σ'
20	20	0.0594
20	25	0.0025
20	30	0.0015
20	35	0.0015
20	40	0.0015
20	45	0.0015
20	50	0.0015
20	55	0.0015
20	60	0.0015
$\lambda = 10$		
μ	N	Relative error on σ'
20	20	0.0618
20	25	0.0310
20	30	0.0309
20	35	0.0311
20	40	0.0307
20	45	0.0031
20	50	0.0008
20	55	0.0008
20	60	0.0008
$\lambda = 20$		

Table 2 gives the relative error on σ' with N increasing, $\mu = 20$, $R_{\text{DOM}} = 2$, and $R_{\text{PML}} - R_{\text{DOM}} = 5h$. We observe that we need to take N large enough to converge to the same level of error as in Table 1, and N needs to be larger for larger λ : $N = 30$ for $\lambda = 10$ and $N = 50$ for $\lambda = 10$. This is consistent with the fact that u and v are more and more oscillatory when λ increases, and we observed numerically that taking $N \sim \lambda$ is sufficient to keep the error bounded independently of λ .

4.3. Main numerical results. The values of σ' in Figure 1 are obtained for $\lambda \geq 3$ with $\mu = 30$, $R_{\text{PML}} - R_{\text{DOM}} = 5h$, and $N = 10\lambda$. For $0.3 \leq \lambda < 3$, we computed σ' , but this required the use of significantly larger μ , usually $\mu = 300$ for $0.3 \leq \lambda \leq 2$ and $\mu = 200$ for $2 \leq \lambda \leq 3$. Figure 2 was produced in the same way, except that we took $\mu = 100$ away from an interval of size 0.2 centered on the quasimode frequencies (which are explicitly computable using the eigenvalues of the Laplacian in the ellipse; see [MGSS22, section 1.1.3]). On the intervals near quasimode frequencies we also needed to increase μ significantly, and we took $\mu = 300$. For every geometry, we refined the mesh around corners in order to obtain good precision.

Acknowledgments. The authors are grateful to Euan Spence for helpful conversations at the beginning of the project and to the anonymous referees for their careful reading and helpful comments.

REFERENCES

- [Am*01] P. R. AMESTOY, I. S. DUFF, J.-Y. L'EXCELLENT, AND J. KOSTER, *A fully asynchronous multifrontal solver using distributed dynamic scheduling*, SIAM J. Matrix Anal. Appl., 23 (2001), pp. 15–41.
- [Am*06] P. R. AMESTOY, A. GUERMOUCHE, J.-Y. L'EXCELLENT, AND S. PRALET, *Hybrid scheduling for the parallel solution of linear systems*, Parallel Comput., 32 (2006), pp. 136–156.

- [Ba*19] S. BALAY, ET AL., *PETSc Users Manual*, ANL-95/11, Revision 3.11, Argonne National Laboratory, 2019.
- [Ba*97] S. BALAY, W. D. GROPP, L. CURFMAN MCINNES, AND B. F. SMITH, *Efficient management of parallelism in object oriented numerical software libraries*, in *Modern Software Tools in Scientific Computing*, E. Arge, A. M. Bruaset, and H. P. Langtangen, eds., Birkhäuser, Basel, 1997, pp. 163–202.
- [BGR82] C. BARDOS, J.-C. GUILLOT, AND J. RALSTON, *La relation de Poisson pour l'équation des ondes dans un ouvert non borné. Application à la théorie de la diffusion*, *Comm. Partial Differential Equations*, 7 (1982), pp. 905–958.
- [Be1994] J.-P. BÉRENGER, *A perfectly matched layer for the absorption of electromagnetic waves*, *J. Comput. Phys.*, 114 (1994), pp. 185–200.
- [Ber*98] A. BERMÚDEZ, L. HERVELLA-NIETO, A. PRIETO, AND R. RODRÍGUEZ, *An exact bounded PML for the Helmholtz equation*, *C. R. Acad. Sci. Paris, Ser. I*, 339 (2004), pp. 803–808.
- [BK62] M. SH BIRMAN AND M. G. KREĪN, *On the theory of wave operators and scattering operators*, *Dokl. Akad. Nauk. SSSR*, 144 (1962), pp. 475–478.
- [Bu75] V. BUSLAEV, *Local spectral asymptotic behavior of the Green's function in exterior problems for the Schrödinger operator*, *Collection of articles dedicated to the memory of Academician V. I. Smirnov. Vestnik Leningrad. Univ. No. 1 Mat. Meh. Astronom. Vyp.*, 1 (1975), pp. 55–60.
- [Ch83] J. CHEEGER, *Spectral geometry of singular Riemannian spaces*, *J. Differential Geom.*, 18 (1983), pp. 575–657.
- [Ch98] T. CHRISTIANSEN, *Spectral asymptotics for compactly supported perturbations of the Laplacian on \mathbb{R}^n* , *Comm. Partial Differential Equations*, 23 (1998), pp. 933–948.
- [ChDa22] T. CHRISTIANSEN AND K. DATCHEV, *Low Energy Scattering Asymptotics for Planar Obstacles*, arXiv:2210.05744, 2022.
- [CoMo98] F. COLLINO AND P. MONK, *The perfectly matched layer in curvilinear coordinates*, *SIAM J. Sci. Comput.*, 19 (1998), pp. 2061–2090.
- [DuWu15] Y. DU AND H. WU, *Preasymptotic error analysis of higher order FEM and CIP-FEM for Helmholtz equation with high wave number*, *SIAM J. Numer. Anal.*, 53 (2015), pp. 782–804.
- [DyGu13] S. DYATLOV AND C. GUILLARMOU, *Scattering phase asymptotics with fractal remainders*, *Comm. Math. Phys.*, 324 (2013), pp. 425–444.
- [DyZw19a] S. DYATLOV AND M. ZWORSKI, *Mathematical Theory of Scattering Resonances*, *Grad. Stud. Math.* 200, AMS, Providence, RI, 2019, <http://math.mit.edu/~dyatlov/res/>.
- [ErGu22] A. ERN AND J.-L. GUERMOND, *Theory and Practice of Finite Elements*, *Appl. Math. Sci.* 159, Springer, New York, 2004.
- [Ha13] H. FRIEDRICH, *Scattering Theory*, *Lecture Notes in Phys.* 872, Springer, Heidelberg, 2013.
- [GLS21] J. GALKOWSKI, D. LAFONTAINE, AND E. SPENCE, *Perfectly-Matched-Layer Truncation Is Exponentially Accurate at High Frequency*, arXiv:2105.07737, 2021.
- [HaZe99] A. HASSELL AND S. ZELDITCH, *Determinants of Laplacians in exterior domains*, *Int. Math. Res. Not. IMRN*, 18 (1999), pp. 971–1004.
- [He12] F. HECHT, *New development in FreeFEM++*, *J. Numer. Math.*, 20 (2012), pp. 251–266.
- [HöI] L. HÖRMANDER, *The Analysis of Linear Partial Differential Operators I. Distribution Theory and Fourier Analysis*, Springer-Verlag, Berlin, 1983.
- [HöIII] L. HÖRMANDER, *The Analysis of Linear Partial Differential Operators III. Pseudo-Differential Operators*, Springer-Verlag, Berlin, 1985.
- [Iv16] V. IVRII, *100 years of Weyl law*, *Bull. Math. Sci.*, 6 (2016), pp. 379–452, <https://link.springer.com/article/10.1007/s13373-016-0089-y>.
- [JeKa78] A. JENSEN AND T. KATO, *Asymptotic behavior of the scattering phase for exterior domains*, *Comm. Partial Differential Equations*, 3 (1978), pp. 1165–1195.
- [Ka78] T. KATO, *Monotonicity theorems in scattering theory*, *Hadronic J.*, 1 (1978), pp. 134–154.
- [LSW21] D. LAFONTAINE, E. SPENCE, AND J. WUNSCH, *For most frequencies, strong trapping has a weak effect in frequency-domain scattering*, *Comm. Pure. Appl. Math.*, 74 (2021), pp. 2025–2063.
- [MaRa78a] A. MAJDA AND J. RALSTON, *An analogue of Weyl's theorem for unbounded domains, I*, *Duke Math. J.*, 45 (1978), pp. 183–196.
- [MaRa78b] A. MAJDA AND J. RALSTON, *An analogue of Weyl's theorem for unbounded domains, II*, *Duke Math. J.*, 45(1978), pp. 513–536.
- [MaRa79] A. MAJDA AND J. RALSTON, *An analogue of Weyl's theorem for unbounded domains, III*, *Duke Math. J.*, 46(1979), pp. 725–731.

- [MGSS22] P. MARCHAND, J. GALKOWSKI, A. SPENCE, AND E. A. SPENCE, *Applying GMRES to the Helmholtz equation with strong trapping: How does the number of iterations depend on the frequency?*, *Adv. Comput. Math.*, 48 (2022).
- [MaRo15] R. MAZZEO AND J. ROWLETT, *A heat trace anomaly on polygons*, *Math. Proc. Cambridge Philos. Soc.*, 159 (1015), pp. 303–319.
- [McG13] I. MCGILLIVRAY, *The spectral shift function for planar obstacle scattering at low energy*, *Math. Nachr.*, 286 (2013), pp. 1208–1239.
- [Me88] R. MELROSE, *Weyl asymptotics for the phase in obstacle scattering*, *Comm. Partial Differential Equations*, 13 (1988), pp. 1431–1439.
- [DLMF] F. W. J. OLVER, A. B. OLDE DAALHUIS, D. W. LOZIER, B. I. SCHNEIDER, R. F. BOISVERT, C. W. CLARK, B. R. MILLER, B. V. SAUNDERS, H. S. COHL, AND M. A. MCCLAINE, EDs., *NIST Digital Library of Mathematical Functions*, Release 1.1.0, 2020, <http://dlmf.nist.gov/>.
- [PePo82] V. PETKOV AND G. POPOV, *Asymptotic behaviour of the scattering phase for nontrapping obstacles*, *Ann. Inst. Fourier (Grenoble)*, 32 (1982), pp. 111–149.
- [PeZw99] V. PETKOV AND M. ZWORSKI, *Breit–Wigner approximation and distribution of resonances*, *Comm. Math. Phys.*, 204 (1999), pp. 329–351.
- [PeZw00] V. PETKOV AND M. ZWORSKI, *Erratum: Breit–Wigner approximation and distribution of resonances*, *Comm. Math. Phys.*, 214 (2000), pp. 733–735.
- [Ra78] J. RALSTON, *The first variation of the scattering matrix: An addendum*, *J. Differential Equations*, 28 (1978), pp. 155–162.
- [Ro94] D. ROBERT, *A trace formula for obstacles problems and applications*, in *Mathematical Results in Quantum Mechanics* (Blossin, 1993), *Oper. Theory Adv. Appl.* 70, Birkhäuser, Basel, 1994, pp. 283–292.
- [SaVa97] YU. SAFAROV AND D. VASSILIEV, *The Asymptotic Distribution of Eigenvalues of Partial Differential Operators*, *Transl. Math. Monogr.* 155, AMS, Providence, RI, 1997.
- [Sa20] J. J. SAKURAI AND J. NAPOLITANO, *Modern Quantum Mechanics*, 3rd ed., Cambridge University Press, Cambridge, UK, 2020.
- [St99] P. STEFANOV, *Quasimodes and resonances: Sharp lower bounds*, *Duke Math. J.*, 99 (1999), pp. 75–92.
- [St01] P. STEFANOV, *Resonance expansions and Rayleigh waves*, *Math. Res. Lett.*, 8 (2001), pp. 107–124.
- [StWa20] A. STROHMAIER AND A. WATERS, *Geometric and obstacle scattering at low energy*, *Comm. Partial Differential Equations*, 45 (2020), pp. 1451–1511.
- [TZ98] S. H. TANG AND M. ZWORSKI, *From quasimodes to resonances*, *Math. Res. Lett.*, 5 (1998), pp. 261–272.
- [Va22] L. VACOSSIN, *Spectral Gap for Obstacle Scattering in Dimension 2*, arXiv:2201.08259, 2022.